New Journal of Physics
The open access journal at the forefront of physics

Deutsche Physikalische Gesellschaft DPG IOP Institute of Physics

PAPER • OPEN ACCESS

Energy current and its statistics in the nonequilibrium spin-boson model: Majorana fermion representation

To cite this article: Bijay Kumar Agarwalla and Dvira Segal 2017 *New J. Phys.* **19** 043030

View the article online for updates and enhancements.

Related content

- Quantum heat transport in a spin-boson nanojunction: Coherent and incoherent mechanisms
  Yue Yang and Chang-Qin Wu
- Qubit absorption refrigerator at strong coupling
  Anqi Mu, Bijay Kumar Agarwalla, Gernot Schaller et al.
- Full-counting statistics of energy transport of molecular junctions in the polaronic regime
  Gaomin Tang, Zhizhou Yu and Jian Wang

Recent citations

- Frequency-dependent current noise in quantum heat transfer: A unified polaron calculation
  Junjie Liu *et al*
- Current in nanojunctions: Effects of reservoir coupling
  Hari Kumar Yadalam and Upendra Harbola
- Heat transport via a local two-state system near thermal equilibrium
  Tsuyoshi Yamamoto *et al*

IOP ebooks™

Bringing you innovative digital publishing with leading voices to create your essential collection of books in STEM research.

Start exploring the collection - download the first chapter of every title for free.

This content was downloaded from IP address 131.169.5.251 on 01/12/2018 at 23:49

New Journal of Physics
The open access journal at the forefront of physics

Deutsche Physikalische Gesellschaft DPG
IOP Institute of Physics

Published in partnership with: Deutsche Physikalische Gesellschaft and the Institute of Physics

OPEN ACCESS

RECEIVED
3 December 2016

REVISED
13 February 2017

ACCEPTED FOR PUBLICATION
13 March 2017

PUBLISHED
28 April 2017

Original content from this work may be used under the terms of the Creative Commons Attribution 3.0 licence.

Any further distribution of this work must maintain attribution to the author(s) and the title of the work, journal citation and DOI.

PAPER

Energy current and its statistics in the nonequilibrium spin-boson model: Majorana fermion representation

Bijay Kumar Agarwalla and Dvira Segal[1]

Chemical Physics Theory Group, Department of Chemistry, and Centre for Quantum Information and Quantum Control, University of Toronto, 80 Saint George St., Toronto, Ontario, M5S 3H6, Canada
[1] Author to whom any correspondence should be addressed

E-mail: dvira.segal@utoronto.ca

Keywords: quantum heat transport, full counting statistics, spin-boson model

Abstract

We study the statistics of thermal energy transfer in the nonequilibrium (two-bath) spin-boson model. This quantum many-body impurity system serves as a canonical model for quantum energy transport. Our method makes use of the Majorana fermion representation for the spin operators, in combination with the Keldysh nonequilibrium Green's function approach. We derive an analytical expression for the cumulant generating function of the model in the steady state limit, and show that it satisfies the Gallavotti–Cohen fluctuation symmetry. We obtain analytical expressions for the heat current and its noise, valid beyond the sequential and the co-tunneling regimes. Our results satisfy the quantum mechanical bound for heat current in interacting nanojunctions. Results are compared with other approximate theories, as well as with a non-interacting model, a fully harmonic thermal junction.

1. Introduction

The spin-boson (SB) model comprises a two-state system (spin) interacting with a dissipative thermal environment, a collection of harmonic modes. It is one of the (conceptually) simplest, yet non-trivial models in the theory of open quantum systems [1, 2]. The model has found diverse applications in condensed phases physics, chemical dynamics, and quantum optics. In particular, it offers a rich platform for studying complex physical processes such as dissipative spin-dynamics [1], charge and energy transfer phenomena in condensed phases [1, 3], Kondo physics [2], and decoherence dynamics of superconducting qubits [2, 4]. In such applications, the spin system can represent donor-acceptor charge states, a magnetic impurity [1], or a truncated harmonic spectrum, mimicking an anharmonic oscillator [5, 6]. The bosonic bath may stand for a collection of lattice phonons, electromagnetic modes, bound electron–hole pairs, and other composite bosonic excitations [1, 2].

Beyond questions over quantum decoherence, dissipation, and thermalization, which can be addressed by the 'canonical' SB model, the two-bath, nonequilibrium spin-boson (NESB) model has been put forward as a minimal model for exploring the fundamentals of thermal energy transfer in anharmonic nano-junctions [5]. When the two reservoirs are maintained at different temperatures—away from linear response (LR)—nonlinear functionality such as the diode effect can develop in the junction [5–9]. More generally, the NESB model serves as a building block for addressing fundamental and practical challenges in thermal conduction in nanoscale gaps [10–14], quantum heat engine operation [14–18], molecular conduction junctions [12, 19–23] and nano-scale energy conversion devices [21, 24].

From the theoretical perspective, the NESB model is an extremely rich platform for studying nonequilibrium quantum physics. One is interested in studying its transport characteristics, including transient dynamics and steady state properties, while covering different regimes: low-to-high temperatures, weak-to-strong system-bath coupling, adiabatic-to-nonadiabatic spin dynamics, with or without a (magnetic) spin biasing field, from LR to the far from equilibrium regime. This challenge could be tackled by extending open

© 2017 IOP Publishing Ltd and Deutsche Physikalische Gesellschaft

quantum system methodologies, previously developed to treat the dissipative dynamics of the (traditional) SB model, to treat the more complicated, nonequilibrium, two-bath version.

Among the techniques developed to study the characteristics of the thermal heat current in the NESB model we recount perturbative quantum master equation tools: Redfield equation [5–7, 9, 25], the noninteracting blip approximation (NIBA) [6, 7, 26], as well as Keldysh nonequilibrium Green's function (NEGF) methods [27, 28]. Furthermore, efforts have been made to go beyond the standard Born–Markov limit, and include higher order co-tunneling processes [29]. In addition, to interpolate between the weak-coupling Born–Markov limit and strong-coupling NIBA—with general spectral functions—a nonequilibrium polaron-transformed Redfield equation method has been recently developed in [30, 31], capturing the full-counting statistics (FCS) of the SB model in the high temperature limit.

Computational studies had further established the non-monotonic behavior of the heat current with the spin-bath coupling energy, including studies based on the multi-layer multi-configuration Hartree approach [32], the iterative influence functional path integral technique (in the spin-fermion representation) [11, 33], Monte Carlo simulations [10], and the hierarchical equation of motion [34, 35].

Beyond the analysis of the thermal conductance or the energy current, in small systems the fluctuations of the current are expected to reveal plethora of information, such as current correlations to all orders [36, 37]. In fact, rather than focusing on the thermal conductance, it is more demanding yet highly profitable to pursue the probability distribution $P_t(Q)$ of the transferred energy Q within a certain interval of time t. This measure is also known as FCS in the context of electron transport. Obtaining the FCS for interacting systems is a highly desirable, yet formidable task. The FCS of the NESB model has been analyzed so far in two different limits: (i) in the sequential tunneling limit i.e., to the lowest order in the system-bath tunneling strength, by employing the Redfield-type quantum master equation approach [17, 26], and (ii) in the strong coupling and/or high temperature regime, following NIBA-type quantum master equations [26, 38]. A theory interpolating these two limits was presented in [30]. However, these studies still miss the low temperature limit [28].

In this paper, we use the Schwinger–Keldysh NEGF approach [39, 40] in combination with the Majorana fermion representation for the system-spin operators, and obtain the cumulant generating function (CGF) of the NESB model beyond the weak spin-bath coupling limit. The crucial impetus to introduce the Majorana representation is that in the fermion representation we are able to use Wick's theorem, thus obtain relevant nonequilibrium spin–spin correlation functions—while including the counting parameter. Moreover, in the Majorana-fermion representation the system-bath coupling Hamiltonian transforms into a relatively simple form, unlike other well known transformations such as the Jordan–Wigner transformation or the polaron transformation. Our results go beyond the sequential and co-tunneling limits. On the other hand, while our result is valid beyond the strict weak-coupling limit, it misses the strong-coupling behavior as received e.g. in [10, 11, 30, 32, 41] using the NIBA method and numerically exact tools. This is because our approach, while relying on an exact expression for the energy current, is limited to the lowest non-zero order of the nonlinear self-energy. The main outcome of our study is an *analytic* expression for the FCS of the NESB model, capturing quantum effects, interactions, and far-from-equilibrium function.

The paper is organized as follows. We introduce the NESB model and the Majorana fermion representation in section 2. In section 3, we present our main results for the CGF, followed by a discussion over different limits and numerical examples. We further compare our expressions to previous theories on the NESB model, and to the harmonic oscillator (HO)-junction model. We present numerical simulations in Sec. 4, and conclude in Sec. 5. The derivation of the CGF is explained in details in the appendix.

2. Model

The NESB model comprises a two-state (spin) system coupled to two bosonic reservoirs ($\nu = L,\ R$), which are maintained at different temperatures. The generic form of the full Hamiltonian is

$$H = \frac{\hbar\omega_0}{2}\sigma_z + \frac{\hbar\Delta}{2}\sigma_x + \sum_{j,\nu}\hbar\omega_{j,\nu}b^\dagger_{j,\nu}b_{j,\nu} + \sigma_z\sum_{j,\nu}\hbar\lambda_{j,\nu}(b_{j,\nu} + b^\dagger_{j,\nu}). \tag{1}$$

Here, σ_i ($i = x,\ y,\ z$) are different components of the Pauli matrix, ω_0 and Δ represents level detuning and the hopping between the spin states, respectively. $b^\dagger_{j,\nu}$ ($b_{j,\nu}$) is the creation (annihilation) operator of the jth phonon mode in the ν-th reservoir. The last term describes the system-bath coupling term with $\lambda_{j,\nu}$ as the coupling strength. For simplicity, we focus here on the unbiased case with degenerate spin levels ($\omega_0 = 0$). Performing a unitary transformation, given by $U = \frac{1}{\sqrt{2}}(\sigma_x + \sigma_z)$, the transformed Hamiltonian reads

$$\bar{H} = \frac{\hbar\Delta}{2}\sigma_z + \sum_{j,\nu}\hbar\omega_{j,\nu}b^\dagger_{j,\nu}b_{j,\nu} + \sigma_x\sum_{j,\nu}\hbar\lambda_{j,\nu}(b_{j,\nu} + b^\dagger_{j,\nu}). \tag{2}$$

We are interested here in obtaining the steady state energy current and its statistics beyond the weak system-bath coupling limit. Unlike the Redfield master equation technique, which captures only resonant energy transfer processes due to its underlying weak coupling approximation [6], the Keldysh NEGF method offers a well established procedure so as to treat the system-bath interaction in a systematic-perturbative way [39, 40]. However, the validity of Wick's theorem is a crucial requirement for practicing the method. Due to the lack of standard bosonic or fermionic commutation relations for spin operators, the NEGF approach is in fact *unsuitable* to be used in the spin representation of the NESB model. However this problem can be avoided by mapping the impurity spin to fermions, using the Majorana-fermion representation [28, 42, 43].

Explicitly, the spin operators can be expressed as $\vec{\sigma} = -\frac{\mathrm{i}}{2}\vec{\eta}\times\vec{\eta}$, i.e.,

$$\sigma_x = -\mathrm{i}\,\eta_y\,\eta_z,\ \ \sigma_y = -\mathrm{i}\eta_z\eta_x,\ \ \sigma_z = -\mathrm{i}\eta_x\eta_y. \tag{3}$$

Majorana fermions' operators satisfy the anti commutation relation, $\{\eta_\alpha,\ \eta_\beta\} = 0$, for $\alpha \neq \beta$, $\eta^2_\alpha = 1$, and unlike the Dirac fermions, they are real $\eta_\alpha = \eta^\dagger_\alpha$. Therefore, these fermions can be constructed in terms of ordinary Dirac fermions (f, g) and their conjugates as

$$\eta_x = (f + f^\dagger),\ \ \eta_y = \mathrm{i}(f^\dagger - f),\quad \eta_z = (g + g^\dagger). \tag{4}$$

In this context, it is important to introduce the so-called *copy-switching operator*

$$\tau_x = -\mathrm{i}\eta_x\eta_y\eta_z, \tag{5}$$

in terms of which the Majorana fermions can be expressed as $\sigma_\alpha = \tau_x\eta_\alpha$. Note that τ_x commutes with all Majorana fermion operators and therefore is a constant of motion. Also, $\tau^2_x = 1$. With the help of this operator, the spin–spin correlator reduces to correlator involving two Majorana fermions

$$\langle\sigma_\alpha(t)\sigma_\beta(t')\rangle = \langle\tau_x(t)\eta_\alpha(t)\tau_x(t')\eta_\beta(t')\rangle = \langle\eta_\alpha(t)\eta_\beta(t')\rangle. \tag{6}$$

In this mixed Majorana–Dirac representation, the full Hamiltonian reads

$$\bar{H} = \frac{\hbar\Delta}{2}\,(1 - 2f^\dagger f) + \sum_{j,\nu}\hbar\omega_{j\nu}b^\dagger_{j,\nu}b_{j,\nu} + (f^\dagger - f)\,\eta_z\,(B_L + B_R), \tag{7}$$

where $B_\nu \equiv \sum_j \hbar\lambda_{j,\nu}(b_{j,\nu} + b^\dagger_{j,\nu})$ is a ν bath operator coupled to the spin system. Note that in this representation, the system-bath coupling term is no longer given in a bilinear form. For later use, we also identify the components of the Hamiltonian as $\bar{H} = H_S + H_L + H_R + H_{\mathrm{SB}}$, with

$$H_S = \frac{\hbar\Delta}{2}\,(1 - 2f^\dagger f),\ \ H_\nu = \sum_j\hbar\omega_{j,\nu}b^\dagger_{j,\nu}b_{j,\nu},\ H_{\mathrm{SB}} = (f^\dagger - f)\,\eta_z\,(B_L + B_R). \tag{8}$$

3. FCS: main results

3.1. Working expressions for the FCS

The complete information over the energy transport statistics can be obtained from the so-called CGF, $\mathcal{G}(\xi)$, for heat exchange. We begin by defining the energy current operator as the rate of change of energy in one of the reservoirs, say L, and write down the energy current as $I_L(t) = -\frac{\mathrm{d}H^H_L(t)}{\mathrm{d}t}$. Below we interchangeably refer to this quantity as 'energy current' or 'heat current'. The operators are written in the Heisenberg picture, and they evolve with respect to the total Hamiltonian $\bar{H}$ in equation (7). Therefore, the total energy change in the L solid within the time interval $t_0 = 0$ to t, where $t_0(t)$ is the initial (final) observation time, is given by the integrated current

$$Q_L(t,\,t_0) = \int_{t_0=0}^{t} I_L(t')\mathrm{d}t' = H_L(0) - H^H_L(t). \tag{9}$$

Following this definition, we write down the characteristic function $\mathcal{Z}(\xi)$ based on the two-time measurement protocol [36, 37],

$$\mathcal{Z}(\xi) = \langle \mathrm{e}^{\mathrm{i}\xi H_L}\,\mathrm{e}^{-\mathrm{i}\xi H^H_L(t)}\rangle = \langle U^\dagger_{\xi/2}(t,\,0)\,U_{-\xi/2}(t,\,0)\rangle,\ = \left\langle T_c\exp\left[-\frac{\mathrm{i}}{\hbar}\int_c H^{\xi(\tau)}_{\mathrm{SB}}(\tau)\mathrm{d}\tau\right]\right\rangle, \tag{10}$$

Here, ξ is the 'counting-field', keeping track of the net amount of energy transferred from the solid L to the spin. $\langle\ldots\rangle$ represents an average with respect to the total density matrix at the initial time, $\rho_T(0)$. We assume a factorized initial state, $\rho_T(0) = \rho_L(0)\otimes\rho_R(0)\otimes\rho_S(0)$, with reservoirs prepared at a canonical state with inverse temperature $\beta_\nu = T^{-1}_\nu\,\mathrm{k}_{\mathrm{B}=1}$, $\rho_\nu(0) = \mathrm{e}^{-\beta_\nu H_\nu}/\,\mathrm{Tr}_\nu[\mathrm{e}^{-\beta_\nu H_\nu}]$, and an arbitrary state for the spin system

$\rho_S(0)$. We also use the definition,

$$U_p(t,\,0) \equiv \mathrm{e}^{\mathrm{i}pH_L}\,\mathrm{e}^{-\mathrm{i}\bar{H}t}\,\mathrm{e}^{-\mathrm{i}pH_L} = \mathrm{e}^{-\mathrm{i}\bar{H}_p t/\hbar}, \tag{11}$$

for the counting field-dependent unitary evolution. Here, $p = \pm\xi/2$ corresponds to the forward and backward evolution branches. Note that due to the measurement protocol, the modified Hamiltonian $\bar{H}_p$ acquires a phase in the system-bath coupling term, modifying only the left-bath operators,

$$\bar{H}_p = \frac{\hbar\Delta}{2}\,(1 - 2f^\dagger f) + \sum_{j,\nu}\hbar\omega_{j,\nu}b^\dagger_{j,\nu}b_{j,\nu} + (f^\dagger - f)\,\eta_z\,(B^p_L + B_R). \tag{12}$$

Here, $B^p_L = \sum_j \hbar\lambda_{j,L}(b_{j,L}\,\mathrm{e}^{-\mathrm{i}p\hbar\omega_{j,L}} + b^\dagger_{j,L}\,\mathrm{e}^{\mathrm{i}p\hbar\omega_{j,L}})$ is the modified bath operator, dressed by the counting field. In the second line of equation (10), the operators are written in the interaction picture with respect to the non-interacting part of the Hamiltonian $H_S + H_L + H_R$. T_c is the contour-ordered operator which orders operators according to their contour time; earlier contour-time operators are placed to the right of later-time terms. In the long time limit, the CGF is defined as

$$\mathcal{G}(\xi) \equiv \lim_{t\to\infty}\frac{1}{t}\ln\mathcal{Z}(\xi) = \lim_{t\to\infty}\frac{1}{t}\sum_{n=1}^{\infty}\frac{(\mathrm{i}\xi)^n}{n!}\langle\langle Q^n\rangle\rangle. \tag{13}$$

Here, $\langle\langle Q^n\rangle\rangle$ represent cumulants. Specifically, the second cumulant is $\langle\langle Q^2\rangle\rangle = \langle Q^2\rangle - \langle Q\rangle^2$. Taking derivatives of the CGF with respect to ξ immediately hands over the current and its higher order fluctuations, or cumulants. However, instead of working with the CGF directly, one can manipulate the so-called generalized current, defined as

$$\mathcal{I}(\xi) \equiv \frac{\partial\mathcal{G}(\xi)}{\partial(\mathrm{i}\xi)}, \tag{14}$$

by following the nonequilibrium version of Feynman–Hellman theorem first introduced by Gogolin *et al* [44]—in the context of counting statistics for charge transport.

Using the NEGF with counting fields as developed in [45], an expression for the generalized energy current can be formally organized as

$$\mathcal{I}(\xi) = \int_{-\infty}^{\infty}\frac{\mathrm{d}\omega}{4\pi}\,\hbar\omega\,[\tilde{\Pi}^{<}_{xx}(\omega)\Sigma^{>}_L(\omega)\mathrm{e}^{-\mathrm{i}\xi\hbar\omega} - \tilde{\Pi}^{>}_{xx}(\omega)\Sigma^{<}_L(\omega)\mathrm{e}^{\mathrm{i}\xi\hbar\omega}]. \tag{15}$$

When $\xi = 0$, this expression reduces to the standard Meir–Wingreen (MW) formula [46] for heat current [27]. The key advantage in treating the generalized current (15), rather than the CGF itself (13), lies in the fact that the problem can be treated with the diagrammatic NEGF technique as developed for the original MW formula without counting fields [47–50]. In the present case, we follow similar steps—for a counting-field dependent (dressed) Hamiltonian.

In equation (15), the symbol tilde represents that operators within the Green's functions evolve with the dressed (counting field-dependent) Hamiltonian $\bar{H}_p$ given in equation (12). $\tilde{\Pi}^{<,>}_{xx}(\omega)$ are the Fourier transformed lesser and greater components of the spin–spin correlators, namely,

$$\begin{aligned}\tilde{\Pi}^{<}_{xx}(t,\,t') &= -\,\mathrm{i}\langle\sigma_x(t')\sigma_x(t)\rangle_\xi,\\ \tilde{\Pi}^{>}_{xx}(t,\,t') &= -\,\mathrm{i}\langle\sigma_x(t)\sigma_x(t')\rangle_\xi.\end{aligned} \tag{16}$$

$\Sigma^{<,>}_\nu(\omega)$ are the self-energy components emerging due to the coupling of the spin to the solids, responsible for transferring energy in and out of the system,

$$\begin{aligned}\Sigma^{<}_\nu(\omega) &= -\,\mathrm{i}\,n_\nu(\omega)\,\Gamma_\nu(\omega),\\ \Sigma^{>}_\nu(\omega) &= -\,\mathrm{i}\,\bar{n}_\nu(\omega)\,\Gamma_\nu(\omega).\end{aligned} \tag{17}$$

Here, $\bar{n}_\nu(\omega) \equiv [1 + n_\nu(\omega)]$ with $n_\nu(\omega) = (\mathrm{e}^{\beta_\nu\hbar\omega} - 1)^{-1}$ as the Bose–Einstein distribution function and $\beta_\nu = 1/T_\nu$ is the inverse temperature. $\Gamma_\nu(\omega) = 2\pi\sum_j \lambda^2_{j,\nu}\,\delta(\omega - \omega_j)$ is the spectral function for the ν reservoir. Note that we write integrals covering negative frequencies, by extending the range of the spectral function while satisfying $\Gamma_\nu(\omega) = -\Gamma_\nu(-\omega)$.

3.2. Main results

To receive the generalized current, our primary objective is to obtain the components $\tilde{\Pi}^{<,>}_{xx}(\omega)$. These terms are obtained using the NEGF method following a first order perturbation expansion with respect to the interaction of the bath with the spin. We summarize here the central results; details are given in the appendix.

The lesser and greater components are obtained to the lowest non-zero order in the nonlinear self-energy. They are given as

$$\tilde{\Pi}^{<}_{xx}(\omega) = -\frac{4i\Delta^2}{\mathcal{D}(\omega,\xi)}(\Gamma_L(\omega)n_L(\omega)e^{i\xi\hbar\omega} + \Gamma_R(\omega)n_R(\omega)), \tag{18}$$

$$\tilde{\Pi}^{>}_{xx}(\omega) = -\frac{4i\Delta^2}{\mathcal{D}(\omega,\xi)}(\Gamma_L(\omega)\bar{n}_L(\omega)e^{-i\xi\hbar\omega} + \Gamma_R(\omega)\bar{n}_R(\omega)), \tag{19}$$

with

$$\mathcal{D}(\omega,\xi) = (\omega^2 - \Delta^2)^2 + \omega^2 M(\omega,\xi). \tag{20}$$

Here $M(\omega,\xi) = C^2(\omega) + 4A(\omega,\xi)$ includes the two terms,

$$\begin{aligned} C(\omega) &= \Gamma_L(\omega)[1 + 2n_L(\omega)] + \Gamma_R(\omega)[1 + 2n_R(\omega)], \\ A(\omega,\xi) &= \Gamma_L(\omega)\Gamma_R(\omega)[n_L(\omega)\,\bar{n}_R(\omega)(e^{i\xi\hbar\omega} - 1) + n_R(\omega)\,\bar{n}_L(\omega)(e^{-i\xi\hbar\omega} - 1)]. \end{aligned} \tag{21}$$

If we eliminate the counting parameter, $\xi = 0$, $\Pi^{<,>}_{xx}(\omega)$ provides the imaginary components of the response function $\Pi^{R}_{xx}(\omega)$,

$$\mathrm{Im}[\Pi^{R}_{xx}(\omega)] = -\frac{2\Delta^2(\Gamma_L(\omega) + \Gamma_L(\omega))}{(\omega^2 - \Delta^2)^2 + \omega^2[\Gamma_L(\omega)(1 + 2n_L(\omega)) + \Gamma_R(\omega)(1 + 2n_R(\omega))]^2}, \tag{22}$$

matching the results of [28].

Using these expressions, the CGF for the NESB model, $\mathcal{G}_{\mathrm{SB}}(\xi) \equiv \int_0^{\xi} d\xi'\,\mathcal{I}(\xi')$, is obtained as

$$\begin{aligned} \mathcal{G}_{\mathrm{SB}}(\xi) = \int_{-\infty}^{\infty}\frac{d\omega}{4\pi}\frac{\Delta^2}{\omega^2}\ln\{1 + \mathcal{T}_{\mathrm{SB}}(\omega;T_L,T_R)[n_L(\omega)\bar{n}_R(\omega) \\ (e^{i\xi\hbar\omega} - 1) + n_R(\omega)\bar{n}_L(\omega)(e^{-i\xi\hbar\omega} - 1)]\}, \end{aligned} \tag{23}$$

with the temperature-dependent transmission function

$$\mathcal{T}_{\mathrm{SB}}(\omega;T_L,T_R) = \frac{4\Gamma_L(\omega)\Gamma_R(\omega)\omega^2}{(\omega^2 - \Delta^2)^2 + \omega^2[\Gamma_L(\omega)(1 + 2n_L(\omega)) + \Gamma_R(\omega)(1 + 2n_R(\omega))]^2}. \tag{24}$$

This expression is valid with an arbitrary form for the spectral function $\Gamma_\nu(\omega)$. The CGF further satisfies the steady state Gallavotti–Cohen fluctuation symmetry, $\mathcal{G}(\xi) = \mathcal{G}(-\xi + i(\beta_R - \beta_L))$ [51]. Equation (23) constitutes the main result of our work.

The cumulants of the energy flux can be readily obtained by taking derivatives of the CGF with respect to the counting field ξ. For example, the heat current and its noise are given by

$$\langle I\rangle_{\mathrm{SB}} \equiv \frac{\partial\mathcal{G}_{\mathrm{SB}}(\xi)}{\partial(i\xi)}\bigg|_{\xi=0} = \int_{-\infty}^{\infty}\frac{d\omega}{4\pi}\frac{\hbar\Delta^2}{\omega}\mathcal{T}_{\mathrm{SB}}(\omega;T_L,T_R)\,[n_L(\omega) - n_R(\omega)], \tag{25}$$

$$\begin{aligned} \langle S\rangle_{\mathrm{SB}} \equiv \frac{\partial^2\mathcal{G}_{\mathrm{SB}}(\xi)}{\partial(i\xi)^2}\bigg|_{\xi=0} = \int_{-\infty}^{\infty}\frac{d\omega}{4\pi}(\hbar\Delta)^2\{-\mathcal{T}^2_{\mathrm{SB}}(\omega;T_L,T_R)[n_L(\omega) - n_R(\omega)]^2 \\ + \mathcal{T}_{\mathrm{SB}}(\omega;T_L,T_R)[n_L(\omega)\bar{n}_R(\omega) + n_R(\omega)\bar{n}_L(\omega)]\}. \end{aligned} \tag{26}$$

The result for the current agrees with the derivation in [28]—once we organize our expressions, $\int_{-\infty}^{\infty} d\omega \ldots \to 2\times\int_0^{\infty} d\omega \ldots$

The procedure followed in our NEGF-Majorana perturbative formalism does not offer a transparent-intuitive understanding over the nature of the approximations involved. However, the CGF in equation (23), and specifically, the energy current in equation (25), allow us to identify processes that are taken into account here: The energy current expression in equation (25) involves an integral over frequencies, with the integrand comprising the difference between Bose–Einstein occupation functions, weighted by an effective temperature-dependent transmission function. Our perturbative technique thus takes into account tunneling processes beyond the resonant (so called sequential tunneling) limit, and beyond the low-temperature co-tunneling limit (see next section for more details). However, our result does not accommodate inelastic, multi-phonon scattering processes— with combination of modes crossing the junction (e.g., one mode comes in, two modes go out). Such high-order scattering processes are expected to be important when the system-bath coupling is strong, and at high temperatures, when many modes in the baths are active. Multi-phonon processes are accounted for e.g. in the polaronic method [6, 7, 26, 30, 31, 38] and in numerically exact simulations [10, 32, 34, 35]. In this respect, we note that the polaron-transformed Redfield equation method [30, 31] nicely interpolates between the weak-coupling (Born–markov) and the strong coupling (NIBA) regimes. However, this treatment does not take include coherent co-tunneling processes.

Why do we capture here scattering effects beyond a low-order system-bath-perturbative quantum master equation, as described e.g. in [5, 6]? Our starting point in the present calculation is equation (15), the generalized MW formula, which is an exact expression [27]. Our perturbative approach is aimed to calculate the ingredients

in the MW formula, which are the various components of spin–spin correlation functions. In contrast, in e.g. [5, 6], we develop a low-order perturbative expression for the energy current itself, resulting in a lower performance. In fact, a similar framework was followed in [27]: the exact MW expression for the energy current was used, but spin–spin correlation functions were evaluated in the limit of weak system-bath coupling—albeit in the so-called Redfield limit. While this NEGF-Redfield calculation shows substantially improved results over low-order QME techniques [5, 6], the method suffers from a fundamental flaw (common to such treatments), as it does not conserve energy. In this regard, it is important to mention that our perturbative technique does not violate energy conservation, and we further manage to organize the CGF in an elegant analytical form, equation (23), which pinpoints on the scattering effects contained in our treatment.

In the next subsection, we discuss interesting limits of the general results.

3.3. Special limits

Incoherent sequential tunneling. When the system-bath coupling is weak and the reservoirs' temperatures are high, $\Gamma_\nu \ll \Delta \ll T_\nu$, the above generating function reduces to the result obtained from the Redfield quantum master equation approach [26], when directly employing the Born–Markov approximation. We now derive this result. Following equation (23), the generalized current can be simplified to

$$\mathcal{I}_{\rm SB}(\xi) = \int_{-\infty}^{\infty} \frac{{\rm d}\omega}{4\pi} \frac{\Delta^2\, M'(\omega,\, \xi)}{(\omega^2 - \Delta^2)^2 + \omega^2 M(\omega,\, \xi)}, \tag{27}$$

where $M'(\omega,\, \xi) = \frac{\partial M(\omega,\xi)}{\partial({\rm i}\xi)}$. To the lowest order $O(\Gamma^2_{L,R})$, working in the limit $\Gamma_\nu \ll \Delta \ll T_\nu$, the poles in the integrand can be approximated by

$$\pm\left\{\Delta \pm \frac{\rm i}{2}\sqrt{M(\Delta,\, \xi)}\right\}. \tag{28}$$

By employing the residue theorem, the integration in equation (27) results in $\mathcal{I}^{\rm weak}_{\rm SB}(\xi) = \frac{1}{2}\frac{\partial\sqrt{M(\xi)}}{\partial({\rm i}\xi)}$ and the generating function reduces to

$$\mathcal{G}^{\rm weak}_{\rm SB}(\xi) = -\frac{1}{2}(C(\Delta) - \sqrt{M(\Delta,\, \xi)}). \tag{29}$$

This expression matches the result obtained in [26]. This CGF also respects the fluctuation symmetry. It immediately yields the heat current in the weak coupling limit [5]

$$\langle I\rangle^{\rm weak}_{\rm SB} = \hbar\Delta \frac{\Gamma_L(\Delta)\Gamma_R(\Delta)[n_L(\Delta) - n_R(\Delta)]}{[\Gamma_L(\Delta)(1 + 2n_L(\Delta))] + [\Gamma_R(\Delta)(1 + 2n_R(\Delta))]}. \tag{30}$$

Co-tunneling. At low temperatures, $\Gamma_\nu \ll T_\nu \leqslant \Delta$, the process of sequential tunneling is exponentially suppressed since incoming phonons are off-resonance—with frequencies below the spin energy gap, $\omega \ll \Delta$. The dominant contribution to the current and higher order fluctuations thus comes from coherent two-phonon co-tunneling processes. In this limit, the transmission function of equation (24) is given by $\mathcal{T}^{\rm co}_{\rm SB}(\omega,\, T_L,\, T_R) \sim 4\Gamma_L(\omega)\Gamma_R(\omega)\omega^2/\Delta^4 \ll 1$. By approximating $\ln(1 + x) \sim x$ for small x, we reduce the CGF of equation (23) to

$$\mathcal{G}^{\rm co}_{\rm SB}(\xi) = \frac{2}{\pi}\int_0^{\omega_h} {\rm d}\omega\, \frac{\Gamma_L(\omega)\Gamma_R(\omega)}{\Delta^2}\,(n_L(\omega)\bar{n}_R(\omega)({\rm e}^{{\rm i}\xi\hbar\omega} - 1) + n_R(\omega)\bar{n}_L(\omega)({\rm e}^{-{\rm i}\xi\hbar\omega} - 1)), \tag{31}$$

with fluctuation symmetry being satisfied. Here, ω_h, the upper limit in the integral, should be determined by the smaller energy scale: temperature, or the cutoff frequency of the baths. The co-tunneling (co) heat current then becomes

$$\langle I\rangle^{\rm co}_{\rm SB} = \frac{2}{\pi}\int_0^{\omega_h} {\rm d}\omega\hbar\omega \frac{\Gamma_L(\omega)\Gamma_R(\omega)}{\Delta^2}[n_L(\omega) - n_R(\omega)]. \tag{32}$$

This expression was previously achieved in two ways: (i) by using a systematic perturbative treatment [25], and (ii) working with the so-called Born–Oppenheimer approach for heat exchange [52], by assuming slow bath and a fast (high frequency) impurity. In the case of an Ohmic bath, $\Gamma_\nu(\omega) \propto \omega^s$ with $s = 1$, the heat current scales as $\langle I\rangle^{\rm co}_{\rm SB} \propto T_L^4 - T_R^4$, thus the thermal conductance scales with T^3, in agreement with numerically exact simulations on the NESB model [10]. As well, in this low temperature limit the NESB junction behaves similarly to a fully harmonic junction, as we discuss in section 3.4.

Note that in contrast to the CGF received in equations (23) and (29), the CGF in the co-tunneling limit is *symmetric* with respect to $\Gamma_\nu(\omega)$. Therefore, in this limit the system does not support the thermal rectification effect. Moreover, in this limit the cumulants $C^n = \frac{\partial^n \mathcal{G}_{\rm SB}(\xi)}{\partial({\rm i}\xi)^n}\Big|_{\xi=0}$ scale as $C^n \propto 1/\Delta^2$, whereas in the sequential tunneling limit cumulants grow as $C^n \propto \Delta^n$.

3.4. Comparison between the NESB model and the HO junction

In the HO junction, a single HO of frequency ω_0, replaces the spin impurity of the NESB model, equation (1). The resulting Hamiltonian is fully harmonic, and it can be readily solved exactly to yield the CGF [53, 54]

$$\mathcal{G}_{\rm HO}(\xi) = -\int_{-\infty}^{\infty}\frac{{\rm d}\omega}{4\pi}\ln\left[1 - \mathcal{T}_{\rm HO}(\omega)(n_L(\omega)\bar{n}_R(\omega)({\rm e}^{{\rm i}\xi\hbar\omega} - 1) + n_R(\omega)\bar{n}_L(\omega)({\rm e}^{-{\rm i}\xi\hbar\omega} - 1))\right]. \tag{33}$$

Surprisingly, our final expression for the CGF of the NESB model, equation (23), is very similar to this expression. The following differences show up: (i) in the HO case the transmission function does not depend on the temperatures of the baths,

$$\mathcal{T}_{\rm HO}(\omega) = \frac{4\,\Gamma_L(\omega)\,\Gamma_R(\omega)\,\omega^2}{(\omega^2 - \omega_0^2)^2 + \omega^2\,(\Gamma_L(\omega) + \Gamma_R(\omega))^2}. \tag{34}$$

Further, (ii) there is a crucial sign difference in this CGF as compared to $\mathcal{G}_{\rm SB}(\xi)$ in equation (23). This sign difference reflects on the nonlinear nature of the spin. A similar sign-difference between harmonic and spin impurity nanojunctions has been observed in vibrationally-assisted electron conducting junctions [21, 24]. The above expression immediately provides the Landauer formula for the heat current,

$$\langle I\rangle_{\rm HO} = \frac{1}{4\pi}\int_{-\infty}^{\infty}{\rm d}\omega\hbar\omega\mathcal{T}_{\rm HO}(\omega)[n_L(\omega) - n_R(\omega)], \tag{35}$$

and the noise

$$\langle S\rangle_{\rm HO} = \frac{1}{4\pi}\int_{-\infty}^{\infty}{\rm d}\omega(\hbar\omega)^2[\mathcal{T}^2_{\rm HO}(\omega)(n_L(\omega) - n_R(\omega))^2 + \mathcal{T}_{\rm HO}(\omega)(n_L(\omega)\bar{n}_R(\omega) + \bar{n}_R(\omega)n_L(\omega))]. \tag{36}$$

In the weak coupling limit, the CGF of the HO model reduces to the standard result obtained by a low order QME [17, 26]

$$\mathcal{G}^{\rm weak}_{\rm HO}(\xi) = \frac{1}{2}\left(C_{\rm HO}(\omega_0) - \sqrt{C^2_{\rm HO}(\omega_0) - 4\,A_{\rm HO}(\omega_0,\,\xi)}\right), \tag{37}$$

with

$$C_{\rm HO}(\omega_0) = \Gamma_L(\omega_0) + \Gamma_R(\omega_0),$$
$$A_{\rm HO}(\omega_0,\,\xi) = \Gamma_L(\omega_0)\Gamma_R(\omega_0)(n_L(\omega_0)\,\bar{n}_R(\omega_0)({\rm e}^{{\rm i}\xi\hbar\omega_0} - 1) + n_R(\omega_0)\,\bar{n}_L(\omega_0)({\rm e}^{-{\rm i}\xi\hbar\omega_0} - 1)).$$

The heat current then reduces to the familiar result,

$$\langle I\rangle^{\rm weak}_{\rm HO} = \hbar\omega_0\frac{\Gamma_L(\omega_0)\Gamma_R(\omega_0)}{\Gamma_L(\omega_0) + \Gamma_R(\omega_0)}[n_L(\omega_0) - n_R(\omega_0)]. \tag{38}$$

The co-tunneling limit is more subtle, and we exemplify it now when calculating the current. We break the transmission function (34) into two contributions (leaving for a moment the numerator) $\mathcal{T}_{\rm HO}(\omega) = \mathcal{T}_o(\omega) + \mathcal{T}_e(\omega)$,

$$\mathcal{T}_o(\omega) = \frac{\omega^2 - \omega_0^2}{(\omega^2 - \omega_0^2)^2 + [\Gamma_L(\omega) + \Gamma_R(\omega)]^2\omega^2},$$
$$\mathcal{T}_e(\omega) = \frac{\omega_0^2}{(\omega^2 - \omega_0^2)^2 + [\Gamma_L(\omega) + \Gamma_R(\omega)]^2\omega^2}. \tag{39}$$

Assuming the hierarchy of energies $\Gamma_\nu \ll T_\nu \leqslant \omega_0$, we note that the function $\omega\,[n_L(\omega) - n_R(\omega)]$ changes slowly at the vicinity of ω_0, in the regime where the functions $\mathcal{T}_{e,o}(\omega)$ have significant weight. Therefore, the integral (35) over the odd component (approximately) cancels out, and the current is solely determined by the even term, $\mathcal{T}_e(\omega) \sim 1/\omega_0^2$, to yield

$$\langle I\rangle^{\rm co}_{\rm HO} = \frac{2}{\pi}\int_0^{\omega_h}{\rm d}\omega\hbar\omega\frac{\Gamma_L(\omega)\Gamma_R(\omega)}{\omega_0^2}[n_L(\omega) - n_R(\omega)]. \tag{40}$$

This result reproduces exactly the behavior of the NESB model in the corresponding limit, equation (32). This correspondence is not surprising: at low temperatures (smaller than the energy spacing in the quantum impurity) and at weak system-bath coupling, the NESB and the HO junctions should behave rather similarly. For a comprehensive analysis of the harmonic-mode thermal junction, see [55].

3.5. Steady state population and a bound on heat current

Besides transport properties, we use the Majorana formalism and calculate the steady state population of the ground and excited states in the eigenbasis of the spin. This can be obtained by calculating $\langle\sigma_z\rangle$ in the transformed basis (2), given as,

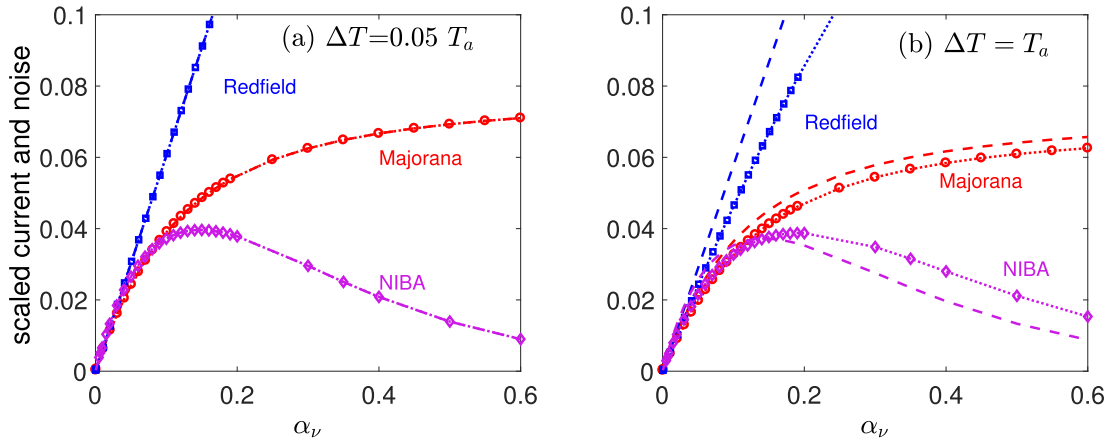

Figure 1. Scaled current $\langle I\rangle/\Delta T$ (dashed lines) and noise $\langle S\rangle/2T_a^2$ (symbols) for the NESB model as a function of coupling strength α_ν, employing different theoretical schemes: Redfield (blue), Majorana (red) and NIBA (purple). (a) Results close to equilibrium, $\Delta T = 0.05T_a$. (b) Calculations far-from-equilibrium, $\Delta T = T_a$, demonstrating deviations from the fluctuation–dissipation theorem. Parameters are $\Delta = T_a = 1$, $T_{L,R} = T_a \pm \Delta T/2$, $\omega_c = 10\Delta$, and $\alpha_L = \alpha_R$.

$$\begin{aligned}\langle\sigma_z\rangle &= \mathrm{i}\int_{-\infty}^{\infty}\frac{\mathrm{d}\omega}{4\pi}\left[(1\ \ 1)G^{>}_{\Psi}(\omega)\begin{pmatrix}1\\-1\end{pmatrix}-(-1\ \ 1)G^{<}_{\Psi}(\omega)\begin{pmatrix}1\\1\end{pmatrix}\right]\\ &= -\frac{\Delta}{\pi}\int_{-\infty}^{\infty}\mathrm{d}\omega\,\omega\,\frac{\Gamma_L(\omega)+\Gamma_R(\omega)}{(\omega^2-\Delta^2)^2+\omega^2\,C^2(\omega)}.\end{aligned}\tag{41}$$

The function $C(\omega)$ is defined in equation (21). In the weak coupling limit, we receive the same result as obtained in [6],

$$\langle\sigma_z\rangle_{\mathrm{weak}} = -\frac{\Gamma_L(\Delta)+\Gamma_R(\Delta)}{\Gamma_L(\Delta)[1+2n_L(\Delta)]+\Gamma_R(\Delta)[1+2n_R(\Delta)]}.\tag{42}$$

The population of the states are $p_g = \frac{1}{2}(1-\langle\sigma_z\rangle)$ and $p_e = \frac{1}{2}(1+\langle\sigma_z\rangle)$.

Recently, a rigorous quantum mechanical bound for the heat current in interacting systems has been derived, valid at the high temperature—yet in the quantum regime [56]. We now confirm that the heat current derived in our work, equation (25), does not violate the bound. This further affirms the validity and usefulness of our result.

In the following analysis we make use of the inequality $0 \leqslant [n_L(\omega)-n_R(\omega)] \leqslant (T_L-T_R)/(\hbar\omega)$ for $\omega > 0$ and $T_L > T_R$. As well, we recall on the positivity of the transmission function $\mathcal{T}_{\mathrm{SB}}(\omega) > 0$. Furthermore, we assume an Ohmic spectral density function for the reservoirs, $\Gamma_\nu(\omega) = \gamma_\nu\,\omega$, $\nu = L,\ R$ (see [56] for a detailed discussion over different spectral functions). Putting these pieces together, we conclude that the heat current of equation (25) satisfies the following inequality

$$\begin{aligned}\langle I\rangle &\leqslant \int_{-\infty}^{\infty}\frac{\mathrm{d}\omega}{4\pi}\,\frac{4\gamma_L\gamma_R\Delta^2\omega^2(T_L-T_R)}{(\omega^2-\Delta^2)^2+\omega^2C^2(\omega)}\\ &= \frac{2}{\pi}\,\Delta^2(T_L-T_R)\frac{\gamma_L\gamma_R}{\gamma_L+\gamma_R}\int_0^{\infty}\mathrm{d}\omega\,\omega^2\frac{\gamma_L+\gamma_R}{(\omega^2-\Delta^2)^2+\omega^2C^2(\omega)}\\ &= -\,\Delta(T_L-T_R)\frac{\gamma_L\gamma_R}{\gamma_L+\gamma_R}\langle\sigma_z\rangle\end{aligned}\tag{43}$$

which precisely matches with the bound organized in [56] for the NESB model. We conclude that our expression for the current thus does not violate a fundamental bound, unlike the prediction of the Redfield QME, see [56].

4. Numerical results

In figures 1–3, we present simulations demonstrating the behavior of the heat current $\langle I\rangle$ and the second cumulant $\langle S\rangle$, based on equation (23), as a function of the system-bath coupling, averaged temperature, and temperature difference. We compare our results to two different methods: the Born–Markov limit, as originally proposed in [5], referred to as 'Redfield', and the high-temperature NIBA equations as developed originally in the same work, referred to as 'NIBA'. For a more recent discussion over these two limits, see [11]. We focus on the following questions regarding the operation of the NESB nanojunction:

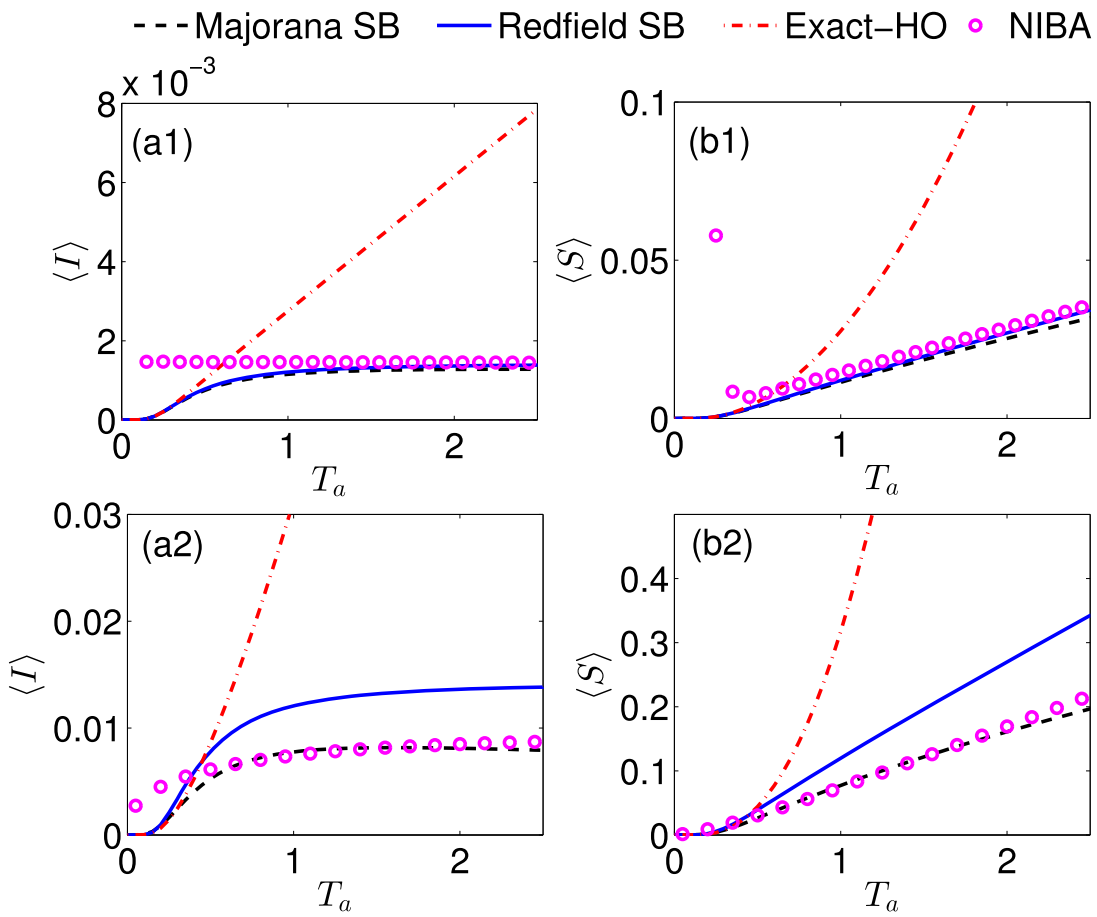

Figure 2. Temperature dependence of the heat current and noise for the SB junction (Redfield, Majorana and NIBA) and the HO model. (a1)–(b1) Weak coupling limit $\alpha_\nu = 0.01$. (a2)–(b2) Intermediate coupling, $\alpha_\nu = 0.1$. Parameters are $\Delta = 1$, $\Delta T = 0.2T_a$ and $T_{L,R} = T_a \pm \Delta T/2$, $\omega_c = 10\Delta$.

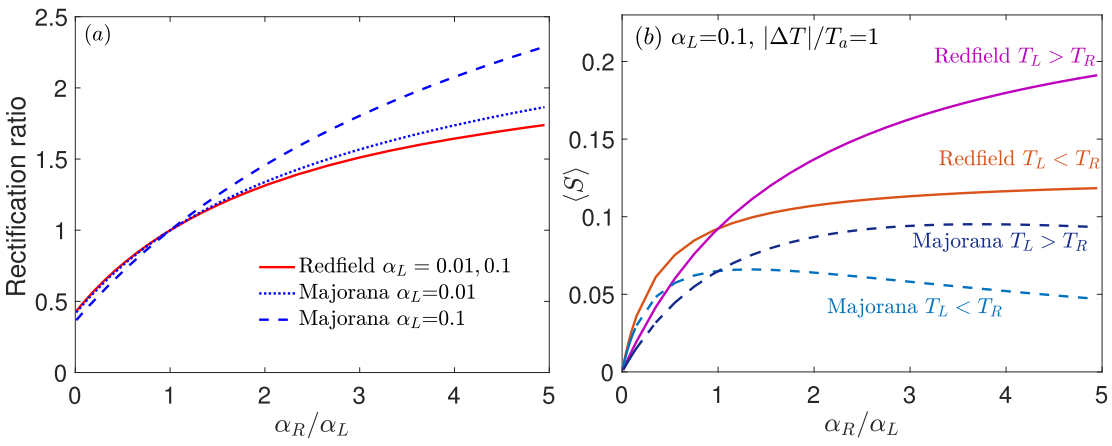

Figure 3. Thermal diode effect. (a) Rectification ratio, $R = \langle I(T_L = 1.5,\ T_R = 0.5)\rangle / |\langle I(T_L = 0.5,\ T_R = 1.5)\rangle|$, as a function of the asymmetry in the system-bath coupling, α_R/α_L, while fixing α_L. (b) Noise $\langle S\rangle$ for forward and backward operations as a function of the junction asymmetry using $\alpha_L = 0.1$. Parameters are $\Delta = 1$, $\Delta T = T_a$, $(T_L,\ T_R)$=(1.5, 0.5) and (0.5, 1.5), $\omega_c = 10\Delta$.

(i) How are the current and noise influenced by the system-bath coupling strength (figures 1 and 3)? (ii) What are the signatures of operating the system far from equilibrium, as opposed to the LR regime (figures 1 and 3)? (iii) What is the temperature dependence of the heat current (figure 2)? (iv) Thermal diode effect: Can we enhance this effect if we go beyond the weak spin-bath coupling (figure 3)? (v) What is the relation between the Majorana-based treatment and other techniques (figures 1–3)?

Figure 1 displays the current and the noise as obtained from equations (25) and (26), as well as the weak coupling (Redfield) limit [11, 26] and the NIBA approximation [11, 41]. Here and below, we use an ohmic spectral function for the baths with an exponential cutoff, $\Gamma_\nu(\omega) = \pi\alpha_\nu\omega e^{-\omega/\omega_c}$. In accord with previous results (for the heat current [11]), we find that Redfield equation dramatically overestimates the current and the noise beyond weak coupling, in comparison to the (more accurate) Majorana and NIBA results. The Majorana treatment shows a saturation of the current and its noise at large α, but under NIBA these quantities quickly decay beyond $\alpha \sim 0.15$. Since the temperature is rather high, $\Delta = T_a$, with $T_a = (T_L + T_R)/2$, we expect the NIBA to be rather accurate here for the ohmic spectral function [10, 11, 41]. Note that our NIBA treatment [11, 26, 41] fails at weak coupling for e.g., a bath characterized by a super-ohmic spectral function, as discussed in [30, 31]. To remedy this problem, a polaron-transformed Redfield equation method was developed in [30], properly capturing both the weak and strong coupling regimes.

We also confirm in figure 1 panel (a) that in LR, the conductance, $\langle I\rangle_{\rm LR}/\Delta T$, is proportional to the thermal noise in the junction, in accord with the Green–Kubo relation,

$$\langle S\rangle_{\rm eq} = 2T_a^2\langle I\rangle_{\rm LR}/\Delta T. \tag{44}$$

Far from equilibrium (see panel (b)), we obviously observe violations of the above relation. However, it is interesting to note that the current and noise still follow a similar functional form within the three different methods.

Figure 2 displays the temperature dependence of the current and the noise. We study both the NESB model and a fully harmonic junction, equations (35) and (36), and make the following observations: (i) comparing the current in the HO and NESB nanojunctions, anharmonicity, as realized here by the spin, leads to the suppression of the heat current. (ii) At weak coupling, $\alpha_\nu = 0.01$, see panels (a1)–(b1), the Majorana and Redfield approaches for the NESB model agree. Results from NIBA agree here as well—at high temperatures, as expected. (iii) Beyond the strict weak coupling limit, $\alpha_\nu = 0.1$, see panels (a2)–(b2), the Redfield formalism leads to unphysical high currents, even beyond the harmonic limit. (iv) At high temperatures and for weak-intermediate couplings, Majorana and NIBA agree, showing the saturation of the current with temperature, see panel (a2) [12].

Next, we discuss the operation of the NESB as a heat diode, as suggested in [5]. To materialize this effect, it is necessary to (i) include anharmonic interactions, and (ii) introduce a spatial asymmetry [8]. The NESB model naturally includes an anharmonic potential. We break here the left–right symmetry by using different coupling strengths at the contacts, $\alpha_L \neq \alpha_R$. In figure 3, we analyze the ratio between the forward and backward currents as we switch the temperatures of the two baths, $R \equiv |\langle I(T_L, T_R)\rangle|/|\langle I(T_R, T_L)\rangle|$. We set $\alpha_L = 0.01, 0.1$, and modify α_R over a broad range of values.

Based on equation (30), we can readily confirm that under the Redfield formalism the rectification ratio R *does not* depend on the absolute value of α (given the linearity of the current with α), only on the ratio α_R/α_L. In contrast, the Majorana treatment, which goes beyond weak coupling, reveals that the diode effect is enhanced as we increase the coupling strength itself. This result points out to the crucial role of many-body interactions in realizing the diode function.

The thermal noise of a rectifying junction is displayed in figure 3(b). For $\alpha_R/\alpha_L > 2$, the Redfield approach, which predicts a lower rectification ratio than the Majorana treatment, suffers from a higher level of noise.

5. Conclusions

We have studied the statistics of energy transfer in the NESB model. By combining Majorana fermion representation for the spin operators with the Schwinger–Keldysh Green's function approach, we were able to derive an analytical expression for the CGF of the model. This function, which we confirmed here to satisfy the fluctuation symmetry for heat exchange, hands over the complete information over the energy statistics in the steady state limit. Our approach goes beyond the weak-coupling (Redfield) and the co-tunneling limits. Surprisingly, the CGF of the NESB model has a similar structure as in the HO junction, besides sign differences and the appearance of a temperature-dependent transmission function—in the NESB model. These differences reflect on the nonlinear nature of the SB system.

We have presented numerical examples for the heat current and its noise, and compared our results to previously-developed quantum master equation approaches, namely Redfield and the NIBA. We have further demonstrated that a heat diode becomes more effective as we increase the system-bath coupling. Additional improvements to the Majorana formulation presented here could be made, e.g., by developing a polaron-transformed Majorana fermion-NEGF approach [57]. Future work will be focused on simulating counting statistics in the NESB model beyond perturbative approaches [35, 58, 59].

Acknowledgments

The work of DS and BKA was supported by an NSERC Discovery Grant, the Canada Research Chair program, and the CQIQC at the University of Toronto.

Appendix. Derivation of the CGF within an NEGF approach

Our goal is to evaluate the generalized current, equation (15). It is given in terms of the (dressed) lesser $\tilde{\Pi}^{<}_{xx}(t,\,t') = -\mathrm{i}\langle\sigma_x(t')\sigma_x(t)\rangle_\xi$ and greater $\tilde{\Pi}^{>}_{xx}(t,\,t') = -\mathrm{i}\langle\sigma_x(t)\sigma_x(t')\rangle_\xi$ correlators. Keeping in mind the nonequilibrium setup, we introduce the ξ-dependent contour-ordered Green's function for the σ_x component,

$$\begin{aligned}\tilde{\Pi}_{xx}(\tau,\,\tau') &= -\,\mathrm{i}\langle T_c\sigma_x(\tau)\sigma_x(\tau')\rangle_\xi \\ &= \begin{bmatrix}\tilde{\Pi}^{t}_{xx}(t,\,t') & \tilde{\Pi}^{<}_{xx}(t,\,t') \\ \tilde{\Pi}^{>}_{xx}(t,\,t') & \tilde{\Pi}^{\bar{t}}_{xx}(t,\,t')\end{bmatrix}.\end{aligned} \tag{A1}$$

Recall that $\langle\cdots\rangle_\xi$ means that operators are evolving with the dressed Hamiltonian of equation (12). Here $\tau,\,\tau'$ are the contour times. When projecting to real time $(t,\,t')$, we receive four different components, namely, time-ordered (t), anti-time ordered $(\bar{t})$, lesser $(<)$ and greater $(>)$ Green's functions.

To evaluate the greater and lesser components, we use the Majorana fermion representation of spin operators, equations (3)–(6). We identify our objective of interest by $-\mathrm{i}\langle T_c\,(f(\tau)+f^\dagger(\tau))(f(\tau')+f^\dagger(\tau'))\rangle_\xi$. We define Green's function for the Dirac f fermion in the Bogolyubov–Nambu representation i.e., $\Psi \equiv (f,\,f^\dagger)^T$ and $\Psi^\dagger \equiv (f^\dagger,\,f)$, and write $\hat{\tilde{G}}_\Psi(\tau,\,\tau') = -\mathrm{i}\langle T_c\Psi(\tau)\Psi(\tau')\rangle_\xi$. The symbol hat in $\hat{\tilde{G}}_\Psi(\tau,\,\tau')$ represents a 2×2 matrix in the contour space (4×4 in real time) i.e.,

$$\hat{\tilde{G}}_\Psi(\tau,\,\tau') = \begin{bmatrix}-\,\mathrm{i}\langle T_c f(\tau)f^\dagger(\tau')\rangle_\xi & -\,\mathrm{i}\langle T_c f(\tau)f(\tau')\rangle_\xi \\ -\,\mathrm{i}\langle T_c f^\dagger(\tau)f^\dagger(\tau')\rangle_\xi & -\,\mathrm{i}\langle T_c f^\dagger(\tau)f(\tau')\rangle_\xi\end{bmatrix} \tag{A2}$$

and in real time

$$\hat{\tilde{G}}_\Psi(t,\,t') = \begin{bmatrix}\tilde{G}^{t}_{\psi}(t,\,t') & \tilde{G}^{<}_{\psi}(t,\,t') \\ \tilde{G}^{>}_{\psi}(t,\,t') & \tilde{G}^{\bar{t}}_{\psi}(t,\,t').\end{bmatrix} \tag{A3}$$

Each component comprises a 2×2 matrix. Then the $\tilde{\Pi}^{<,>}_{xx}(\omega)$ components can be alternatively expressed as

$$\begin{aligned}\tilde{\Pi}^{<}_{xx}(\omega) &= -(1\;\;1)\,\tilde{G}^{<}_{\Psi}(\omega)\begin{pmatrix}1\\1\end{pmatrix}, \\ \tilde{\Pi}^{>}_{xx}(\omega) &= (1\;\;1)\,\tilde{G}^{>}_{\Psi}(\omega)\begin{pmatrix}1\\1\end{pmatrix}.\end{aligned} \tag{A4}$$

We next construct a Dyson (kinetic) equation for $\hat{\tilde{G}}_\Psi(\tau,\,\tau')$ following the dressed Hamiltonian in equation (12) treating the nonlinear part of the Hamiltonian, $(f^\dagger - f)\eta_z(B^p_L + B_R)$, as a perturbation,

$$\hat{\tilde{G}}_\Psi(\tau,\,\tau') = \hat{G}_{\Psi,0}(\tau,\,\tau') + \int \mathrm{d}\tau_1 \int \mathrm{d}\tau_2 \hat{G}_{\Psi,0}(\tau,\,\tau_1)\,\hat{\tilde{\Sigma}}_\Psi(\tau_1,\,\tau_2)\,\hat{\tilde{G}}_\Psi(\tau_2,\,\tau'). \tag{A5}$$

The Green's functions of the ordinary fermion g and the reservoirs operators are calculated to the lowest (noninteracting) order. We thus write the contour ordered version of the self-energy $\hat{\tilde{\Sigma}}_\Psi(\tau_1,\,\tau_2)$ as

$$\hat{\tilde{\Sigma}}_\Psi(\tau,\,\tau') = \mathrm{i}\hat{\lambda}(\tilde{\Sigma}_L(\tau,\,\tau') + \Sigma_R(\tau,\,\tau'))\,G_\eta(\tau,\,\tau'). \tag{A6}$$

$\hat{G}_{\Psi,0}(\tau,\,\tau')$ is the Green's function corresponding to the the noninteracting part of the Hamiltonian. It satisfies the following differential equation in contour time

$$(\mathrm{i}\partial_\tau\hat{I} - \Delta\hat{\sigma}_z)\hat{G}_{\Psi,0}(\tau,\,\tau') = \hat{\delta}(\tau-\tau'), \tag{A7}$$

where $\hat{I}$ is 2×2 identity matrix. In frequency domain, we obtain the solution $\hat{G}^{-1}_{\Psi,0}(\omega) = \mathrm{diag}(\omega-\Delta,\,\omega+\Delta,\,-\omega+\Delta,\,-\omega-\Delta)$.

In equation (A6), $G_\eta(\tau,\,\tau') = -\mathrm{i}\langle T_c\eta_z(\tau)\eta_z(\tau')\rangle$ is the Green's function involving the zth component of the Majorana fermion, $\hat{\lambda}$ is the Nambu matrix

$$\hat{\lambda} = \begin{bmatrix}1 & -1\\ -1 & 1\end{bmatrix} \tag{A8}$$

and $\tilde{\Sigma}_L$, Σ_R are the bare Green's functions for the Bosonic baths,

$$\tilde{\Sigma}_L(\tau,\tau') = -\,\mathrm{i}\langle \tilde{B}_L(\tau)\,\tilde{B}_L(\tau')\rangle,$$
$$\Sigma_R(\tau,\tau') = -\,\mathrm{i}\langle B_R(\tau)\,B_R(\tau')\rangle, \tag{A9}$$

Recall that the operators of the left reservoirs are dressed by the additional ξ dependence, i.e., $\tilde{B}_L(\tau) = B_L^{-\xi/2}(t)$ ($B_L^{+\xi/2}(t)$), when τ is on the upper (lower) branch. Given the perturbative nature of our treatment, the self-energy contribution from the baths is additive.

To the lowest non-zero order, various components of the self-energy can be obtained analytically. Invoking the steady state limit, we write down these components in frequency domain, given by the convolution of the Green's functions for the baths and the Majorana fermions. Following equation (A6), we get

$$\tilde{\Sigma}_\Psi^{>,<}(\omega) = \mathrm{i}\hat{\lambda}\int\frac{\mathrm{d}\omega'}{2\pi}\tilde{\Sigma}_X^{>,<}(\omega-\omega')\,G_\eta^{>,<}(\omega'), \tag{A10}$$

where we use the notation $\tilde{\Sigma}_X^{>,<} = \tilde{\Sigma}_L^{>,<} + \Sigma_R^{>,<}$. This expression can be further simplified by using symmetry relations, as follows. The sum and difference of the lesser and greater components are given by

$$\tilde{\Sigma}_\Psi^K(\omega) = \frac{\mathrm{i}\hat{\lambda}}{2}\int\frac{\mathrm{d}\omega'}{2\pi}[(\tilde{\Sigma}_X^{>} - \tilde{\Sigma}_X^{<})(\omega+\omega')(G_\eta^r(\omega') - G_\eta^a(\omega')) - \tilde{\Sigma}_X^K(\omega+\omega')G_\eta^K(\omega')] \tag{A11}$$

and

$$\tilde{\Sigma}_\Psi^{>}(\omega) - \tilde{\Sigma}_\Psi^{<}(\omega) = \frac{\mathrm{i}\hat{\lambda}}{2}\int\frac{\mathrm{d}\omega'}{2\pi}[\tilde{\Sigma}_X^K(\omega+\omega')(G_\eta^r(\omega') - G_\eta^a(\omega')) - (\tilde{\Sigma}_X^{>}(\omega+\omega') - \tilde{\Sigma}_X^{<}(\omega+\omega'))G_\eta^K(\omega')]. \tag{A12}$$

Here K is the Keldysh component, the sum of lesser and greater Green's functions. The spectral function of the ordinary fermion, $\Gamma_\eta(\omega) = \frac{\mathrm{i}}{2}(G_\eta^r(\omega) - G_\eta^a(\omega)) = 2\pi\delta(\omega)$, satisfies the regular sum rule $\int\frac{\mathrm{d}\omega}{2\pi}\Gamma_\eta(\omega) = 1$. We also use the effective fluctuation–dissipation relation i.e., $G_\eta^K(\omega) = h_\eta(\omega)\,(G_\eta^r(\omega) - G_\eta^a(\omega)) \propto h_\eta(\omega)\delta(\omega) = 0$ where $h_\eta(\omega) = \tanh(\frac{\beta_L\hbar\omega}{2}) + \tanh(\frac{\beta_R\hbar\omega}{2})$. Putting these pieces together, we obtain simplified expressions for the self-energy components, expressed solely in terms of the reservoirs' self-energies,

$$\tilde{\Sigma}_\Psi^{>}(\omega) = \hat{\lambda}\,\tilde{\Sigma}_X^{>}(\omega), \quad \tilde{\Sigma}_\Psi^{<}(\omega) = -\hat{\lambda}\,\tilde{\Sigma}_X^{<}(\omega). \tag{A13}$$

We next look at the time ordered and anti-time ordered components. These terms are ξ-independent, and they satisfy the following relations

$$\Sigma_\Psi^t(\omega) + \Sigma_\Psi^{\bar{t}}(\omega) = \Sigma_\Psi^{>}(\omega) + \Sigma_\Psi^{<}(\omega) = \hat{\lambda}\,(\Sigma_X^r(\omega) - \Sigma_X^a(\omega)), \tag{A14}$$

$$\Sigma_\Psi^t(\omega) - \Sigma_\Psi^{\bar{t}}(\omega) = \frac{\mathrm{i}\hat{\lambda}}{2}\int\frac{\mathrm{d}\omega}{2\pi}\Sigma_X^K(\omega)(G_\eta^r(\omega) + G_\eta^a(\omega)) = 0. \tag{A15}$$

To derive the last expression, we ignore the lamb shift part. We therefore find that

$$\Sigma_\Psi^t(\omega) = \Sigma_\Psi^{\bar{t}}(\omega) = -\frac{\mathrm{i}\hat{\lambda}}{2}(\Gamma_L(\omega) + \Gamma_R(\omega)), \tag{A16}$$

where $\Gamma_\nu(\omega) = \mathrm{i}(\Sigma_\nu^r(\omega) - \Sigma_\nu^a(\omega))$ describes the reservoir-subsystem coupling energy. Therefore, to the lowest order in perturbation theory, the self-energy $\hat{\bar{\Sigma}}_\Psi$ is fully determined by the reservoir's Green's functions as given by equations (A13) and (A16).

We can now solve equation (A5), by projecting it to real time then Fourier transforming it,

$$\bar{\tilde{G}}_\Psi^{-1}(\omega) = \bar{G}_{\Psi,0}^{-1}(\omega) - \bar{\tilde{\Sigma}}_\Psi(\omega)$$
$$= \begin{bmatrix} \omega-\Delta+\frac{\mathrm{i}}{2}\Gamma(\omega) & -\frac{\mathrm{i}}{2}\Gamma(\omega) & \tilde{\Sigma}_X^{<}(\omega) & -\tilde{\Sigma}_X^{<}(\omega) \\ -\frac{\mathrm{i}}{2}\Gamma(\omega) & \omega+\Delta+\frac{\mathrm{i}}{2}\Gamma(\omega) & -\tilde{\Sigma}_X^{<}(\omega) & \tilde{\Sigma}_X^{<}(\omega) \\ \tilde{\Sigma}_X^{>}(\omega) & -\tilde{\Sigma}_X^{>}(\omega) & \omega-\Delta-\frac{\mathrm{i}}{2}\Gamma(\omega) & \frac{\mathrm{i}}{2}\Gamma(\omega) \\ -\tilde{\Sigma}_X^{>}(\omega) & \tilde{\Sigma}_X^{>}(\omega) & \frac{\mathrm{i}}{2}\Gamma(\omega) & \omega+\Delta-\frac{\mathrm{i}}{2}\Gamma(\omega) \end{bmatrix}. \tag{A17}$$

Here, the symbol bar represents $\bar{A} = \hat{\sigma}_z A$ with $\hat{\sigma}_z = \mathrm{diag}(1,\,1,\,-1,\,-1)$, introduced so as to take into account the appropriate signs for upper and lower branches of the contour. $\Gamma(\omega) = \Gamma_L(\omega) + \Gamma_R(\omega)$. Inverting this matrix we obtain the lesser component

$$\tilde{G}^{<}_{\Psi}(\omega) = \frac{1}{\mathcal{D}(\omega,\,\xi)}\begin{bmatrix}(\omega+\Delta)^2\,\tilde{\Sigma}^{<}_{X}(\omega) & -(\omega^2-\Delta^2)\,\tilde{\Sigma}^{<}_{X}(\omega)\\ -(\omega^2-\Delta^2)\,\tilde{\Sigma}^{<}_{X}(\omega) & (\omega-\Delta)^2\,\tilde{\Sigma}^{<}_{X}(\omega)\end{bmatrix}, \tag{A18}$$

and the greater component

$$\tilde{G}^{>}_{\Psi}(\omega) = -\frac{1}{\mathcal{D}(\omega,\,\xi)}\begin{bmatrix}(\omega+\Delta)^2\,\tilde{\Sigma}^{>}_{X}(\omega) & -(\omega^2-\Delta^2)\,\tilde{\Sigma}^{>}_{X}(\omega)\\ -(\omega^2-\Delta^2)\,\tilde{\Sigma}^{>}_{X}(\omega) & (\omega-\Delta)^2\,\tilde{\Sigma}^{>}_{X}(\omega)\end{bmatrix}. \tag{A19}$$

$\mathcal{D}(\omega,\,\xi)$ is the determinant of the matrix, given as

$$\begin{aligned}\mathcal{D}(\omega,\,\xi) = {} & (\omega^2-\Delta^2)^2+\omega^2[(\Gamma_L(\omega)(1+2n_L(\omega))+\Gamma_R(\omega)(1+2n_R(\omega)))^2+4\Gamma_L(\omega)\Gamma_R(\omega)\{n_L(\omega)\bar{n}_R(\omega)\\ & (e^{i\xi\hbar\omega}-1)+n_R(\omega)\bar{n}_L(\omega)(e^{-i\xi\hbar\omega}-1)\}].\end{aligned} \tag{A20}$$

with $\bar{n}_\nu(\omega) = 1 + n_\nu(\omega)$. Using equation (A4), the lesser and greater components of spin–spin correlation functions are finally obtained as

$$\begin{aligned}\tilde{\Pi}^{<}_{xx}(\omega) &= -\frac{4i\Delta^2}{\mathcal{D}(\omega,\,\xi)}(\Gamma_L(\omega)n_L(\omega)e^{i\xi\hbar\omega}+\Gamma_R(\omega)n_R(\omega)),\\ \tilde{\Pi}^{>}_{xx}(\omega) &= -\frac{4i\Delta^2}{\mathcal{D}(\omega,\,\xi)}(\Gamma_L(\omega)\bar{n}_L(\omega)e^{-i\xi\hbar\omega}+\Gamma_R(\omega)\bar{n}_R(\omega)).\end{aligned} \tag{A21}$$

Substituting these expressions into the generalized current expression, equation (15), we receive

$$\mathcal{I}(\xi) = \int_{-\infty}^{\infty}\frac{d\omega}{4\pi}\frac{\Delta^2}{\omega^2}\frac{1}{\mathcal{D}(\omega,\,\xi)}\frac{\partial}{\partial(i\xi)}[\mathcal{D}(\omega,\,\xi)]. \tag{A22}$$

Manipulating it as $\mathcal{G}(\xi) = \int_0^{\xi}\mathcal{I}(\xi')d\xi'$, we get

$$\mathcal{G}(\xi) = \int_{-\infty}^{\infty}\frac{d\omega}{4\pi}\frac{\Delta^2}{\omega^2}\ln\left[\frac{\mathcal{D}(\omega,\,\xi)}{\mathcal{D}(\omega,\,\xi=0)}\right], \tag{A23}$$

which we organize into our main result, equation (23).

References

[1] Weiss U 1999 *Quantum Dissipative Systems* (Singapore: World Scientific)
[2] Leggett A J, Chakravarty S, Dorsey A T, Fisher M P A, Garg A and Zwerger W 1987 *Rev. Mod. Phys.* **59** 1
[3] Nitzan A 2006 *Chemical Dynamics in Condensed Phases* (New York: Oxford University Press)
[4] Le Hur K 2010 *Understanding Quantum Phase Transitions* ed L D Carr (Boca Raton: Taylor and Francis)
[5] Segal D and Nitzan A 2005 *Phys. Rev. Lett.* **94** 034301
[6] Segal D 2006 *Phys. Rev.* B **73** 205415
[7] Segal D and Nitzan A 2005 *J. Chem. Phys.* **122** 194704
[8] Wu L-A and Segal D 2009 *Phys. Rev. Lett.* **102** 095503
[9] Wu L-A, Yu C X and Segal D 2009 *Phys. Rev.* E **80** 041103
[10] Saito K and Kato T 2013 *Phys. Rev. Lett.* **111** 214301
[11] Boudjada N and Segal D 2014 *J. Phys. Chem.* A **118** 11323
[12] Segal D and Agarwalla B K 2016 *Annu. Rev. Phys. Chem.* **67** 185
[13] Wang J-S, Wang J and Lu J T 2008 *Eur. Phys. J.* B **62** 381
[14] Li N *et al* 2012 *Rev. Mod. Phys.* **84** 1045
[15] Segal D and Nitzan A 2006 *Phys. Rev.* E **73** 026109
[16] Segal D 2008 *Phys. Rev. Lett.* **101** 260601
[17] Ren J, Hänggi P and Li B 2010 *Phys. Rev. Lett.* **104** 170601
[18] Chen T, Wang B X and Ren J 2013 *Phys. Rev.* B **87** 144303
[19] Simine L and Segal D 2012 *Phys. Chem. Chem. Phys.* **14** 13820
[20] Simine L and Segal D 2014 *J. Chem. Phys.* **141** 014704
[21] Agarwalla B K, Jiang J-H and Segal D 2015 *Phys. Rev.* B **92** 245418
[22] Cuevas J C and Scheer E 2010 *Molecular Electronics: An Introduction to Theory and Experiment* (Singapore: World Scientific)
[23] Galperin M, Ratner M A and Nitzan A 2007 *J. Phys.: Condens. Matter* **19** 103201
[24] Agarwalla B K, Jiang J-H and Segal D 2015 *Beilstein J. Nanotechnol.* **6** 2129
[25] Ruokola T and Ojanen T 2011 *Phys. Rev.* B **83** 045417
[26] Nicolin L and Segal D 2011 *J. Chem. Phys.* **135** 164106
[27] Velizhanin K A, Thoss M and Wang H 2010 *J. Chem. Phys.* **133** 084503
[28] Yang Y and Wu C Q 2014 *Euro. Phys. Lett* **107** 30003
[29] Thingna J, Zhou H and Wang J S 2014 *J. Chem. Phys.* **141** 194101
[30] Wang C, Ren J and Cao J 2015 *Sci. Rep.* **5** 11787
[31] Wang C, Ren J and Cao J 2017 *Phys. Rev. A* **95** 023610
[32] Velizhanin K A, Wang H and Thoss M 2008 *Chem. Phys. Lett.* **460** 325
[33] Segal D 2013 *Phys. Rev.* B **87** 195436
[34] Kato A and Tanimura Y 2015 *J. Chem. Phys.* **143** 064107

[35] Cerrillo J, Buser M and Brandes T 2016 *Phys. Rev.* B **94** 214308
[36] Esposito M, Harbola U and Mukamel S 2009 *Rev. Mod. Phys.* **81** 1665
[37] Campisi M, Hänggi P and Talkner P 2011 *Rev. Mod. Phys.* **83** 771
[38] Nicolin L and Segal D 2011 *Phys. Rev.* B **84** 161414
[39] Rammer J 2007 *Quantum Field Theory of Non-Equilibrium States* (Cambridge: Cambridge University Press)
[40] Wang J-S, Agarwalla B K, Li H and Thingna J 2014 *Front. Phys.* **9** 673
[41] Segal D 2014 *Phys. Rev.* E **90** 012148
[42] Shnirman A and Makhlin Y 2003 *Phys. Rev. Lett.* **91** 207204
[43] Mao W, Coleman P, Hooley C and Langreth D 2003 *Phys. Rev. Lett.* **91** 207203
[44] Gogolin A O and Komnik A 2006 *Phys. Rev.* B **73** 195301
[45] Li H, Agarwalla B K, Li B and Wang J-S 2013 *Eur. Phys. J.* B **86** 500
[46] Meir Y and Wingreen N 1992 *Phys. Rev. Lett.* **68** 2512
[47] Schwinger J 1961 Brownian motion of a quantum oscillator *J. Math. Phys.* **2** 407
[48] Kadanoff L P and Baym G 1962 *Quantum Statistical Mechanics* (New York: Benjamin-Cummings)
[49] Keldysh L V 1965 Diagram technique for nonequilibrium processes *Sov. Phys.—JETP* **20** 1018
[50] Danielewicz P 1984 Quantum theory of nonequilibrium processes: I *Ann. Phys.* **152** 239
[51] Gallavotti G and Cohen E G D 1995 *Phys. Rev. Lett.* **74** 2694
[52] Wu L-A and Segal D 2011 *Phys. Rev.* E **83** 051114
[53] Saito K and Dhar A 2007 *Phys. Rev. Lett.* **99** 180601
[54] Agarwalla B K, Li B and Wang J-S 2012 *Phys. Rev.* E **85** 051142
[55] Vinkler-Aviv Y, Schiller A and Andrei N 2014 *Phys. Rev.* B **89** 024307
[56] Taylor E and Segal D 2015 *Phys. Rev. Lett.* **114** 220401
[57] Liu J, Xu H and Wu C-Q 2016 *Chem. Phys.* **481** 42
[58] Carrega M, Solinas P, Braggio A, Sassetti M and Weiss U 2015 *New J. Phys.* **17** 045030
[59] Carrega M, Solinas P, Sassetti M and Weiss U 2016 *Phys. Rev. Lett.* **116** 240403